

# Neutral and Charged Polymer Brushes: A Model Unifying Curvature Effects from Micelles to Flat Surfaces

C. Biver,<sup>†</sup> R. Hariharan,<sup>‡</sup> J. Mays,<sup>§</sup> and W. B. Russel<sup>\* ,⊥</sup>

Centre d'Application de Levallois, Elf Atochem, BP 108, 92300 Levallois-Perret, France, Research and Development Center, General Electric Company, Schenectady, New York 12301, Department of Chemistry, University of Alabama, Birmingham, Alabama 35294-1240, and Department of Chemical Engineering, Princeton University, Princeton, New Jersey 08544

Received July 11, 1996; Revised Manuscript Received December 20, 1996<sup>®</sup>

**ABSTRACT:** Conformations of neutral and charged brushes on spheres have been explored for diblock and triblock copolymers adsorbed on colloidal particles and associated in micelles. The variation of layer thickness  $L$  with adsorbed amount for a wide range of core radii  $R$  ( $0.04 < L/R < 20$ ) agrees well with the blob model of Daoud and Cotton for neutral polymers and a new "electrostatic blob model" for semirigid polyelectrolytes. The latter combines the Daoud and Cotton model with the electrostatic wormlike chain theory for polyelectrolytes to account for chain stiffening and excluded volume interactions inside the blobs.

## Introduction

A wide variety of polymers are used to stabilize colloidal particles. When adsorbed or grafted at interfaces, they create a repulsive potential that can dominate the attractive van der Waals forces responsible for aggregation, particularly when the polymer layer is thick, dense, and effectively adsorbed irreversibly.<sup>1</sup> Thus predicting the conformation of polymer brushes at interfaces is of considerable importance with respect to colloidal stability. The conformation of neutral polymer brushes on flat or curved surfaces has been widely investigated both theoretically<sup>2–5</sup> and experimentally,<sup>6,7</sup> but relatively less work has been directed toward the conformation when the solvated block is a polyelectrolyte.<sup>8–11</sup> In this case, repulsive interactions due to the charges along the polymer backbone add to the entropic and excluded volume contributions to the free energy, resulting in improved stability.

An important parameter governing polymer chain conformation on a colloidal sphere is the dimensionless curvature usually expressed as  $L/R$ , where  $L$  is the thickness of the polymer layer and  $R$  the particle radius. Increasing the surface curvature reduces segment–segment interactions in the polymer layer, which should result in an increase in surface coverage and a decrease in layer thickness.<sup>12</sup> A particularly strong effect of curvature is expected for polyelectrolytes due to the electrostatic contributions to the segment–segment interactions.

In this paper, we propose a model that accounts for local chain stiffening and electrostatic excluded volume more effectively than previous attempts and reconciles variations in the adsorbed amount and layer thickness for a wide range of curvatures and systems: coated particles and micelles, neutral and charged brushes. The simple blob picture, introduced by Daoud and Cotton<sup>13</sup> for neutral star polymers was already applied to micelles in solution,<sup>4,10</sup> end-functionalized neutral polymer chains adsorbed at spherical interfaces,<sup>12</sup> and charged diblock copolymers aggregated in micelles or adsorbed

on curved interfaces,<sup>7,8</sup> but to our knowledge, the theoretical predictions have not been validated by experiments for either neutral or charged diblock copolymers.

In the following sections, we first recall the results of the main theoretical and experimental studies dealing with the effects of surface curvature. Then we describe the Daoud–Cotton model as modified for the coated particle and micelle cases and the main features of the Yamakawa et al.<sup>17–19</sup> and the wormlike chain theories<sup>21–24</sup> for modeling segment–segment interactions in neutral and charged polymer brushes, respectively. With the concept of an electrostatic wormlike chain, we extend the Daoud–Cotton model (DCM) to polyelectrolytes grafted on a sphere, as the electrostatic blob model (EBM), which incorporates the theory of dilute polyelectrolyte solutions introduced by Odijk<sup>20,21</sup> and Fixman<sup>22,23</sup> and implemented by Davis and Russel.<sup>24</sup> This treatment applies at concentrations below the semidilute regime for semirigid polyelectrolytes, with Kuhn lengths greater than the geometric mean of the Bjerrum length  $l_b$  and the spacing between charges.<sup>25–27</sup> For poly(styrenesulfonate), the polyelectrolyte of interest here, the persistence length and Bjerrum length are comparable, so we adopt the semirigid chain as a reasonable model. The former assumption may need further consideration, since brushes generate considerable interactions between chains. The EBM and DCM then serve to correlate experimental data for polyelectrolyte diblock copolymers in micelles or coating particles and neutral triblock copolymers with an adsorbing midblock. For polyelectrolytes, we restrict our attention to highly charged chains at concentrations of added salt much higher than the concentration of counterions associated with the fixed charges. We find that the models serve to unify data from our experiments<sup>28</sup> and others in the literature,<sup>29,30</sup> over a wide range of radii of curvature for neutral and charged brushes on coated particles and micelles.

## Background

Theoretical works predict the effect of curvature on the adsorbed amount and the layer thickness for neutral polymers. Ligoure and Leibler<sup>16</sup> considered the adsorption of end-functionalized polymers on spherical par-

<sup>†</sup> Elf Atochem.

<sup>‡</sup> General Electric Company.

<sup>§</sup> University of Alabama.

<sup>⊥</sup> Princeton University.

<sup>®</sup> Abstract published in *Advance ACS Abstracts*, March 1, 1997.

ticles and predicted a monotonous decrease of the surface coverage with increasing particle size. By comparing the free energy of diblock copolymer chains aggregated in micelles or adsorbed on colloidal particles, Qiu and Wang<sup>31</sup> showed that increasing the size of the colloidal particle encourages the polymer chains to form micelles instead of adsorbing on the particles, consistent with the Ligoure and Leibler theory.

Experimental data covering a very wide range of  $L/R$  are available for adsorbed brushes on nanometric size particles and flat surfaces. For the adsorption of triblock copolymers of poly(ethylene oxide)–poly(propylene oxide)–poly(ethylene oxide) (PEO–PPO–PEO) on polystyrene latices, Li et al.<sup>29</sup> found a systematic increase in the surface coverage with the particle size in contrast with the theoretical predictions. Our work<sup>28</sup> examined the adsorption of diblock polyelectrolyte copolymers of poly(*tert*-butylstyrene)–sodium poly(styrenesulfonate) (PtBS–PSS) on polystyrene latices but found no clear trends for either the adsorbed amount or the layer thickness as a function of the particle size. Merrington et al.<sup>33</sup> studied the adsorption of end-functionalized polystyrene from toluene on monodisperse silica particles, finding no systematic trend for the adsorbed amount as a function of particle size; they did not measure layer thicknesses. Only Singh et al.<sup>34</sup> offer data that agree with theory. For end-functionalized polystyrene adsorbed on colloidal silica beads on Al-coated silicon substrates, the surface coverage decreased systematically with increasing particle size until interactions between layers on adjacent particles become significant.

In most of these studies, an increase in the layer thickness with the particle size is usually observed in agreement with theoretical predictions. However, no common trend emerges regarding the influence of curvature on adsorbed amount. This unexpected experimental result probably reflects a change in the surface properties with particle size.

## Theory

**Excluded Volume Interactions.** The renormalization group approach<sup>35</sup> describes chains at interfaces as a succession of blobs, beyond which segment–segment interactions are screened. By definition, the chain within one blob assumes a conformation equivalent to that in a dilute polymer solution, with monomers interacting with both adjacent and distant segments in the blob but not with segments from other blobs. The interactions inside one blob can thus be described by two parameters: the statistical segment length  $l$ , which accounts for interactions between adjacent monomers and characterizes the local chain stiffness, and the excluded volume  $v/\beta$ , which characterizes interactions between distant segments along the chain. For neutral polymers, only the latter depends on the polymer–solvent affinity and contributes to chain expansion, but for polyelectrolytes, electrostatic interactions affect both and through them the coil size.

For neutral polymer brushes, we adopt the approach outlined by Yamakawa and Stockmayer<sup>19</sup> for dilute solutions to describe the interactions inside one blob. In this case, local chain stiffening due to steric hindrance is accommodated through the characteristic ratio  $C_\infty$ , which determines the length of a statistical segment as  $l = C_\infty l_0$ , where  $l_0$  is the contour length per bond. The architecture of the backbone primarily determines  $C_\infty$ .<sup>28</sup> The number of statistical segments  $N$  is obtained by

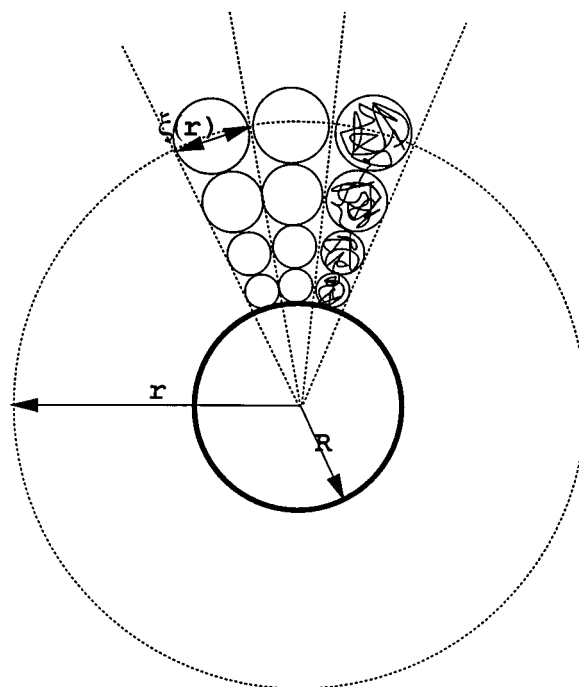


**Figure 1.** Blob model for grafted or adsorbed polymer chains on a sphere of radius  $R$  and for polymer chains aggregated in micelles with core radius  $R$ .

preserving the polymer contour length as  $Nl = N_0 l_0$ , with  $N_0$  being the number of bonds per chain.

In good solvents, excluded volume causes the chain to expand beyond its ideal dimension under  $\theta$  conditions. Though more accurate theories exist, e.g., Yamakawa and Tanaka<sup>17</sup> and Yamakawa and Stockmayer,<sup>19</sup> we adopt the Flory<sup>36</sup> result for the radius of gyration,

$$R_g = 0.41 \left( \frac{v}{\beta} \right)^{1/5} N^{3/5} l \quad (1)$$

which is roughly equivalent in the good solvent limit. This allows us to estimate the excluded volume  $v/\beta$  from measured hydrodynamic radii for isolated homopolymer chains comparable to the nonadsorbing blocks of the copolymers.

**Daoud and Cotton Model (DCM).** This approach accounts for curvature by considering chains of  $N$  statistical segments of length  $l$  aggregated in a micelle of core radius  $R$  or adsorbed/grafted on a particle of radius  $R$ . The number of chains per micelle is defined as the aggregation number  $p$ . For a particle, the number of adsorbed chains follows from the adsorbed amount  $\Gamma$  [kg/m<sup>2</sup>] as

$$p = 4\pi R^2 \frac{N_a \Gamma}{M_w} \quad (2)$$

where  $M_w$  is the total molecular weight of the adsorbed polymer and  $N_a$  is Avogadro's number, which also determine the dimensionless chain density,

$$\sigma = \frac{N_a \Gamma}{M_w} \quad (3)$$

The basic hypothesis of the DCM is that chains at a spherical interface form radial branches, consisting of a succession of close packed blobs with size  $\xi(r)$  such that (Figure 1)

$$p\pi\xi^2(r)/4 = 4\pi r^2 \quad (4)$$

The Flory theory for good solvents relates the number of segments  $N_\xi$  to  $\xi$  through<sup>35</sup>

$$\xi \approx N_\xi^{3/5} l \left( \frac{v}{f} \right)^{1/5} \quad (5)$$

Thus, the excluded volumes extracted via (1) are employed in the same context. From the segment density inside a blob,  $\rho = 6N_\xi/\pi\xi^3$ , the total number of segments within the adsorbed layer of thickness  $L$  follows as

$$\rho N = 4\pi \int_R^{R+L} r^2 \rho(r) dr \quad (6)$$

Evaluation of this integral leads to the prediction that a polymer brush in a good solvent extends from the surface a distance  $L$  given by

$$\left( \frac{L}{R} + 1 \right)^{5/3} = 1 + k \frac{Nl}{R} \left( \frac{\sigma v}{f} \right)^{1/3} \quad (7)$$

where  $k = O(1)$  is a constant.

We tested the prediction above and found linear variations of  $(L/R + 1)^{5/3}$  with  $Nl\sigma^{1/3}/R$  for two sets of experimental data: ours<sup>28</sup> for PtBS/PSS diblocks adsorbed on polystyrene particles ( $0.65 < L/R < 1.7$ ) from a  $10^{-1}$  M NaCl solution and a second for PEO/PPO/PEO triblocks adsorbed on polystyrene particles ( $0.04 < L/R < 0.09$ ) from water<sup>29</sup>. The diblock copolymer has a polyelectrolyte solvated block, whereas the triblock copolymer is neutral; thus, the slopes, which are proportional to  $v/f$ , differ. This suggests correlating the two by estimating the excluded volume parameters.

**Electrostatic Wormlike Chains.** For polyelectrolytes, local chain stiffening arises from both steric hindrances and electrostatic repulsions. Thus, changes in the ionic strength cause remarkable variations in the local stiffness as well as in the excluded volume. We adopt the electrostatic wormlike chain theory for strongly charged polyelectrolytes, which predicts quantitatively the radii of gyration and second virial coefficients of potassium poly(styrenesulfonate) over a broad range of ionic strengths.<sup>39</sup>

This theory replaces the real chain by an equivalent chain of  $N_k$  statistical segments, each of length  $l_k$ , while conserving the contour length of the chain. To account for electrostatic effects within each segment, Fixman<sup>23</sup> modeled a section of the backbone as a charged torus and solved the nonlinear Poisson–Boltzmann equation for the electrostatic field. Balancing the electrostatic and steric hindrance energy against the kinetic energy  $kT$  then determines the electrostatic Kuhn length  $l_k$ , which reduces to  $l$  in the absence of electrostatic interactions. The excluded volume parameter  $v$ , which depends on  $l_k$  and the ionic strength, characterizes the segment–segment interactions. Davis and Russel<sup>24</sup> summarized calculations for  $l_k$  and  $v$  for poly(styrene-sulfonate) for a wide range of ionic strengths. Subsequent analysis<sup>25</sup> has validated this approach for semirigid polyelectrolytes with  $l \gg 2l_b/f$  where  $l_b$  and  $l/f$  are the Bjerrum length and the spacing between charges, respectively. For fully sulfonated polystyrene,  $l_b = 0.125$  nm and  $C_\infty = 7.85$ <sup>37</sup> so that  $l = 0.990$  nm and  $1/f = 2l_b/l = 0.25$ . This means that the highly but not fully sulfonated polystyrenes described below have  $l > 2l_b/f \approx 0.41$  nm but not by an order of magnitude. Nonetheless, we consider this sufficient and proceed on the basis

**Table 1. Molecular Characteristics of Symmetric PEO–PPO–PEO Triblock Copolymers<sup>a,29</sup>**

| polymer | $M_{\text{PPO}}$ , kg/mol | $M_{\text{PEO}}$ , kg/mol | $L_c$ , nm |
|---------|---------------------------|---------------------------|------------|
| P105    | 3.2                       | 1.6                       | 13.3       |
| F68     | 1.7                       | 3.3                       | 27.3       |
| F88     | 2.3                       | 4.6                       | 37.4       |
| F108    | 3.2                       | 5.7                       | 46         |

<sup>a</sup> The polydispersity  $M_w/M_n$  is estimated to be less than 1.2.  $L_c$  is the contour length of the PEO chain.

**Table 2. Molecular Characteristics of PtBS–PSS Diblock Polyelectrolytes<sup>a</sup>**

| polymer | $M_{\text{PtBS}}$ , kg/mol | $M_{\text{PSS}}$ , kg/mol | $M_w/M_n$ | $f_0$ | $L_c$ , nm |
|---------|----------------------------|---------------------------|-----------|-------|------------|
| MT3     | 4.31                       | 145.7                     | 1.04      | 0.87  | 191        |
| MT2     | 4.20                       | 83.0                      | 1.03      | 0.89  | 102        |

<sup>a</sup>  $f_0 = 2f_0/l$  is the fraction of sulfonated monomers.<sup>40</sup>  $L_c$  is the contour length of the polyelectrolyte chain.

of the earlier satisfactory results from the theory for the chains in dilute solutions.

Within a polyelectrolyte brush, the layer thickness follows (3) and (7), with  $l_k$ ,  $N_k$ , and  $v$  depending on the ionic strength. The effect of curvature is displayed more clearly with (7) rewritten in the form

$$\frac{L}{L_{\max}} = \left[ \left( 1 + \frac{5}{3} \frac{L_{\max}}{R} \right)^{3/5} - 1 \right] \frac{R}{L_{\max}} \quad (8)$$

with the limit for flat plates determined as  $L_{\max} = (3/5)kNl(\sigma v/f)^{1/3}$  by the mean field theory of Alexander<sup>2</sup> and de Gennes.<sup>3</sup> Thus, for a specific polymer molecular weight and surface density,  $L$  should scale as  $R^{2/5}$  for highly curved interfaces ( $R \ll L_{\max}$ ), while  $L - L_{\max}$  should scale as  $R^{-1}$  for  $R \gg L_{\max}$ .

## Experimental Systems and Procedures

Coated colloidal particles and micelles were examined to check the predictive ability of (7) for neutral polymer and polyelectrolyte brushes. All the brushes examined have high surface coverages as assumed in the DCM. In each case, hydrodynamic layer thicknesses were measured by dynamic light scattering.

**Neutral Polymer Brushes.** Li et al.<sup>29</sup> adsorbed triblock copolymers of PEO/PPO/PEO on polystyrene latices (Table 1) via the hydrophobic PPO midblock, leaving the PEO end blocks solvated. For the PEO,  $l_b = 0.120$  nm and  $C_\infty = 3.8$ .<sup>37</sup> The latex diameters of 69, 130, 212, and 272 nm yielded the surface coverages and layer thicknesses in Figures 3 and 4 of Li et al. Here, a measured surface coverage reduces to  $\sigma = 2N_a fT/M_w$ , since each triblock contributes two chains to the brush. The radii of gyration of the PEO homopolymers reported determine the excluded volume  $v/f = 1.75$  from (1).

**Polyelectrolyte Brushes.** Mays and Chen<sup>40</sup> synthesized diblock copolymers containing a PtBS hydrophobic anchor block and a NaPSS polyelectrolyte block, which constitutes the charged brushes. As shown in Table 2, these polymers have nearly equal hydrophobic block sizes, but MT3 has roughly twice the hydrophilic block size as MT2.

**MT3 Adsorbed on Polystyrene Latices.** We measured both surface coverages and layer thicknesses<sup>28</sup> for the adsorption of MT3 at  $10^{-1}$  M NaCl on latices of four diameters, 91, 137, 202, and 301 nm, and also at  $10^{-4}$ – $10^{-1}$  M NaCl for the 137-nm particles.

**MT2 Micelles.** Guenoun et al.<sup>41</sup> reported micelle formation of MT2 with a critical micellar concentration of the order of  $2 \times 10^{-3}$  kg/m<sup>3</sup> and micellar sizes and aggregation numbers<sup>30</sup> for ionic strengths from  $10^{-2}$  to 0.5 M.

**MT3 Micelles.** We reported<sup>28</sup> micellar sizes for MT3 for added salt concentrations from  $7 \times 10^{-6}$  to  $10^{-1}$  M. The aggregation number in doubly distilled deionized water of 22.6,

**Table 3. (a) Calculated Parameters from the Daoud and Cotton Model and the Flory Theory for Polystyrene Particles coated with PEO–PPO–PEO Copolymers<sup>22</sup> and (b) Calculated Parameters from the Electrostatic Blob Model for Polystyrene Particles Coated with Diblock Polyelectrolyte MT3, MT2 Micelles, and MT3 Micelles**

| polymer   | $R$ , nm | $L$ , nm | $p$    | $\xi_{\min}$ , nm | $\xi_{\max}$ , nm | $N_{\xi_{\min}}$  | $N_{\xi_{\max}}$  | $\bar{N}_b$      | $L_{\max}$ , nm  |             |
|-----------|----------|----------|--------|-------------------|-------------------|-------------------|-------------------|------------------|------------------|-------------|
| Section a |          |          |        |                   |                   |                   |                   |                  |                  |             |
| P105      | 35       | 2.5      | 1 370  | 3.8               | 3.9               | 30                | 28                | 0.7              | 2.6              |             |
|           | 65       | 4.3      | 24 600 | 1.7               | 1.7               | 7                 | 8                 | 2.4              | 4.4              |             |
|           | 106      | 4.1      | 56 600 | 1.8               | 1.8               | 8                 | 9                 | 2.3              | 4.2              |             |
| F68       | 35       | 3.5      | 1 520  | 3.7               | 3.7               | 28                | 27                | 0.9              | 5.5              |             |
|           | 65       | 6.0      | 7 440  | 3.1               | 3.2               | 20                | 21                | 1.9              | 6.1              |             |
|           | 106      | 9.7      | 20 500 | 3.0               | 3.2               | 19                | 21                | 3.1              | 6.1              |             |
| F88       | 136      | 8.1      | 51 600 | 2.4               | 2.5               | 13                | 14                | 3.3              | 7.1              |             |
|           | 35       | 6.0      | 1 370  | 3.9               | 4.2               | 30                | 33                | 1.5              | 7.2              |             |
|           | 65       | 7.0      | 7 950  | 3.0               | 3.2               | 19                | 21                | 2.3              | 8.5              |             |
| F108      | 106      | 10.2     | 23 200 | 2.8               | 3.8               | 17                | 28                | 3.1              | 8.8              |             |
|           | 136      | 9.1      | 52 800 | 2.4               | 2.5               | 13                | 14                | 3.7              | 9.8              |             |
|           | 35       | 6.6      | 1 520  | 3.7               | 4.0               | 28                | 31                | 1.7              | 9.2              |             |
|           | 65       | 8.0      | 8 460  | 2.9               | 3.1               | 18                | 20                | 2.7              | 11.0             |             |
|           | 106      | 11.0     | 31 400 | 2.4               | 2.6               | 13                | 15                | 4.4              | 12.0             |             |
|           | 136      | 14.0     | 59 500 | 2.3               | 2.4               | 12                | 14                | 6.0              | 13.0             |             |
| polymer   | $R$ , nm | $L$ , nm | $p$    | $l_k$ , nm        | $\nu/l_k^3$       | $\xi_{\min}$ , nm | $\xi_{\max}$ , nm | $N_{\xi_{\min}}$ | $N_{\xi_{\max}}$ | $\bar{N}_b$ |
| PS/MT3    | 68.5     | 61.1     | 456    | 5.8               | 1.04              | 14.2              | 22                | 4                | 9                | 3.4         |
|           | 68.5     | 42.2     | 472    | 3.5               | 0.59              | 13.9              | 19                | 12               | 20               | 2.6         |
|           | 45.5     | 73.9     | 233    | 5.8               | 1.04              | 13.7              | 28                | 4                | 13               | 3.6         |
|           | 101.0    | 110.0    | 2,140  | 5.8               | 1.04              | 9.1               | 18                | 2.1              | 6                | 8.2         |
|           | 151.0    | 104.0    | 3,920  | 5.8               | 1.04              | 9.9               | 16                | 2.4              | 6                | 8.1         |
| MT3       | 3.2      | 63.7     | 17     | 10.8              | 1.38              | 6.0               | 44                | 0.3              | 9                | 2.6         |
|           | 3.1      | 59.5     | 16     | 9.0               | 1.33              | 6.4               | 42                | 0.5              | 12               | 2.5         |
|           | 2.8      | 52.1     | 12     | 5.8               | 1.04              | 8.0               | 41                | 1.7              | 25               | 2.2         |
| MT2       | 3.2      | 30.7     | 19     | 5.8               | 1.23              | 5.5               | 21                | 0.9              | 8                | 2.3         |
|           | 3.0      | 24.9     | 16     | 4.4               | 0.91              | 6.1               | 19                | 1.8              | 11               | 2.0         |
|           | 3.0      | 23.0     | 15     | 3.9               | 0.78              | 6.3               | 18                | 2.4              | 13               | 1.9         |

and those from Guenoun et al.<sup>30</sup> for MT2 obey the Wittmer and Joanny<sup>43</sup> prediction

$$p \approx \frac{M_{\text{PtBS}}^{2/3}}{M_{\text{PSS}} f^{4/3}} \quad (9)$$

where *f* is the fraction of charged monomers on the polyelectrolyte block. We estimate the aggregation number of MT3 from (9) and values from Guenoun et al.<sup>30</sup> for MT2 at the ionic strengths of interest here, even though the theory strictly applies only for deionized solutions.<sup>42</sup> The radii of the micellar cores follow from

$$R = \left( \frac{3pM_{\text{PtBS}}}{4\pi N_a \rho_{\text{PtBS}}} \right)^{1/3} \quad (10)$$

where  $\rho_{\text{PtBS}} = 950 \text{ kg/m}^3$  is the bulk density, so the uncertainty in *p* from (9) affects both  $\sigma$  and *R*.

Estimating the electrostatic Kuhn length and excluded volume requires knowledge of the ionic strength *I* inside the brush. In this paper, we limit our treatment to relatively high added salt concentrations ( $1.6 \times 10^{-2}$  to 1 M) for which the counterions from the fixed charges on the polyelectrolyte are negligible. A more careful treatment essential for lower ionic strengths will be the subject of a subsequent paper.<sup>44</sup> *l<sub>k</sub>* and  $\nu$  are obtained for the ionic strengths and molecular weights of interest by interpolating the numerical results of Davis and Russel.<sup>39</sup>

## Results and Discussion

Application of the DCM and EBM expression (7) to neutral or charged brushes differs only in whether the parameters accounting for the interactions on the right hand side include electrostatic effects or not. Thus, a master curve should exist for both neutral and charged brushes, if one accounts correctly for the interactions. To check the universality, we plot  $(L/R + 1)^{5/3} - 1$  vs  $Nl(\sigma\nu/l_k^3)^{1/3}/R$  for the neutral brushes and vs  $N_k l_k(\sigma_k\nu/l_k^3)^{1/3}/R$  for the polyelectrolyte brushes, for  $2.8 \text{ nm} < R < 150.5 \text{ nm}$  and  $0.04 < L/R < 20$  in Figure 2. In this

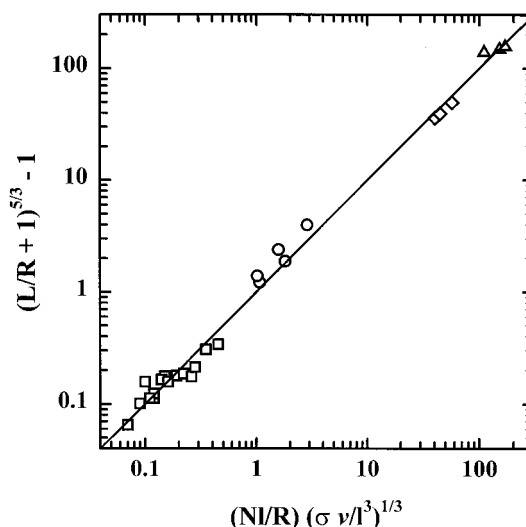


**Figure 2.** Comparison of the model (solid line) with experimental data for neutral brushes of PEO–PPO–PEO triblock copolymers on polystyrene particles<sup>29</sup> (□) and polyelectrolyte brushes consisting of polystyrene particles coated by PtBS–PSS (MT3) diblock copolymers<sup>28</sup> (○), MT3 micelles<sup>28</sup> (△), and MT2 micelles<sup>30</sup> (◇). The horizontal axis refers to  $Nl(\sigma\nu/l_k^3)^{1/3}/R$  for the neutral brushes and  $N_k l_k(\sigma_k\nu/l_k^3)^{1/3}/R$  for the polyelectrolyte brushes.

log–log plot, the experimental points for all the systems fall around a straight line with a zero intercept and a slope of unity. The logarithmic scale tends to exaggerate the quality of the fit; however, the deviations are typically smaller than 30%, which could be attributed to experimental errors and uncertainty in the parameters that enter the calculations. Table 3 also records the sizes and number of segments in the inner and outer blobs for each layer, as well as the approximate number of blobs per chain. The sizes of the first and last blobs in each chain must account for the center being  $\xi/2$  from the edge of the layer. The first or smallest is  $\xi_{\min}$

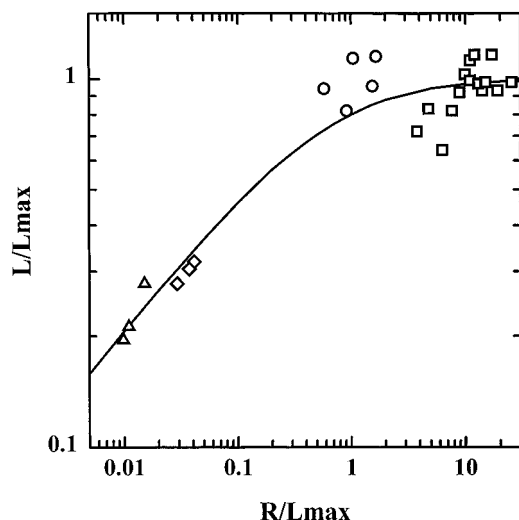


**Figure 3.** Comparison of the nondimensional representation of the model (solid line) in the form of (8) with experimental data for neutral and polyelectrolyte brushes. The experimental data are the same as in Figure 2.

$= 4R/(p^{1/2} - 2)$  and the last, or largest, is  $\xi_{\max} = 4(R + L)/(p^{1/2} + 2)$  with  $N_{\xi_{\min}}$  and  $N_{\xi_{\max}}$  following from (5). The number of blobs per chain can be estimated from the layer thickness and average blob size as  $\bar{N}_b = 2L/(\xi_{\min} + \xi_{\max})$ .

In all cases, the chains contain at least one blob, and the outermost blob incorporates a respectable number of segments. However, the inner most blob of the polyelectrolyte brushes is always deficient in segments, i.e., contains too few to satisfy the presumptions of the blob model. Likewise, the micellar brushes generally contain a small number of blobs, whereas Daoud and Cotton presumed the contrary. Nonetheless, we feel comfortable with the model since the larger blobs comprise the bulk of those layers containing a minimal number and, thereby, determine the thickness  $L$  of primary interest. In addition, the model reduces smoothly to a sphere of individual swollen coils when  $R \rightarrow \infty$  with  $\sigma = 1/N^{6/5}(\nu/\beta)^{2/5}$ , meaning the area per chain corresponds to that for an individual swollen coil in solution. Thus, neither deficiencies in the treatment of the inner part of the layer nor a small number of blobs per chain should invalidate the model.

The ability of the EBM to correlate data over a wide range of curvatures implies the following:

(1) The nonlinear electrostatic theory accurately captures the interactions inside the polyelectrolyte brushes via  $l_k$  and  $\nu$  in the high salt regime.

(2) The curvature dependence is in essence captured by the idea that the blobs grow radially outwards and fill space.

Data for the neutral polymers extend satisfactorily the correlation to lower curvatures, indicating that the Flory theory for the coil dimension of homopolymers in good solvents accounts accurately for excluded volume interactions in neutral brushes.

The alternative plot of  $L/L_{\max}$  vs  $R/L_{\max}$  suggested by (8) shows more clearly the effect of curvature (Figure 3) and the  $\pm 30\%$  deviation. The MT3 micelles have the highest curvature [ $R/L_{\max} = O(10^{-2})$ ], closely followed by MT2 [ $R/L_{\max} = O(3 \times 10^{-2})$ ]. At the other extreme, the PEO-PPO-PEO brushes are almost flat [ $R/L_{\max} = O(10)$ ], with values of  $L/L_{\max}$  close to unity. The particle radii for the PSS polyelectrolyte brushes lie in the same range as the PEO brushes, but the higher

molecular weights and better solvency of the polyelectrolyte block generate larger values of  $L_{\max}$  and lower  $R/L_{\max}$ . At comparable area per chain, the PSS chain dimension in micelles would be smaller (by a factor of 4–5) than on almost flat surfaces. Chain dimensions deviate significantly from the planar limit only when  $L_{\max}$  significantly exceeds  $R$ .

## Conclusions

The blob model of Daoud and Cotton successfully correlates layer thickness and adsorbed amounts of neutral and charged block copolymers on spheres for systems ranging from micelles to coated particles. For polyelectrolyte brushes, we propose an electrostatic blob model, which combines the Daoud and Cotton model with the nonlinear electrostatic theory for dilute polyelectrolyte solutions. This model differs fundamentally from the electrostatic blob model of de Gennes,<sup>36</sup> which pertains to weakly charged polyelectrolytes with charges spaced many Kuhn lengths apart. Our experimental data conform reasonably well with this new model, indicating a faithful representation of chain stiffening and electrostatic excluded volume interactions in the high salt regime, despite the presence of blobs containing a modest number of statistical segments.

**Acknowledgment.** We thank P. Guenoun, G. Chauveteau, and M. Tirrell for many fruitful discussions and K. Caldwell for kindly providing us their preprint. Elf Aquitaine, Elf Atochem, and the National Science Foundation through NSF/CTS-9107025 and the MRSEC/DMR-9400362 are gratefully acknowledged for their financial support.

## References and Notes

- (1) Napper, D. H. *Polymeric Stabilisation of Colloidal Dispersions*; Academic Press: New York, 1983.
- (2) Alexander, S. J. *Phys. Paris* **1977**, 38, 983.
- (3) de Gennes, P. G. *Macromolecules* **1980**, 13, 1069.
- (4) Marques, C.; Joanny, J. F.; Leibler, L. *Macromolecules* **1988**, 21, 1051.
- (5) Milner, S. T.; Witten, T. A.; Cates, M. E. *Macromolecules* **1988**, 21, 2610.
- (6) Patel, S. S.; Tirrell, M. *Annu. Rev. Phys. Chem.* **1989**, 40, 597.
- (7) Halperin, A.; Tirrell, M.; Lodge, T. P. *Adv. Polym. Sci.* **1992**, 100, 31.
- (8) Misra, S.; Varanasi, S.; Varanasi, P. P. *Macromolecules* **1989**, 22, 4173.
- (9) Pincus, P. *Macromolecules* **1991**, 24, 2912.
- (10) Israels, R.; Leermakers, F. A. M.; Fleer, G. J.; Zhulina, E. B. *Macromolecules* **1994**, 27, 3249.
- (11) Borisov, O. V.; Zhulina, E. B.; Birshtein, T. M. *Macromolecules* **1994**, 27, 4795.
- (12) Dan, N.; Tirrell, M. *Macromolecules* **1993**, 26, 4310.
- (13) Daoud, M.; Cotton, J. P. *J. Phys. Paris* **1982**, 43, 531.
- (14) Halperin, A. *Macromolecules* **1987**, 20, 2943.
- (15) Witten, T. A.; Pincus, P. A. *Macromolecules* **1986**, 19, 2509.
- (16) Ligoure, C.; Leibler, L. *Macromolecules* **1990**, 23, 5044.
- (17) Yamakawa, H.; Tanaka, G. *J. Chem. Phys.* **1967**, 47, 3991.
- (18) Yamakawa, H. *Modern Theory of Polymer Solutions*; Harper and Row: New York, 1971.
- (19) Yamakawa, H.; Stockmayer, W. J. *Chem. Phys.* **1972**, 57, 2843.
- (20) Odijk, T. *J. Polym. Sci., Polym. Phys. Ed.* **1977**, 15, 477.
- (21) Odijk, T.; Houwaart, A. C. *J. Polym. Sci., Polym. Phys. Ed.* **1978**, 16, 627.
- (22) Fixman, M.; Skolnick, J. *Macromolecules* **1978**, 11, 863.
- (23) Fixman, M. *J. Chem. Phys.* **1982**, 76, 6346.
- (24) Davis, R. M.; Russel, W. B. *J. Polym. Sci., Polym. Phys.* **1986**, 24, 511.
- (25) Barrat, J. L.; Joanny, J.-F. *Europhys. Lett* **1993**, 24, 333.
- (26) Barrat, J. L.; Joanny, J.-F. *J. Phys. II Fr.* **1994**, 4, 1089.
- (27) Witten, T. A.; Pincus, P. A. *J. Phys. II Fr.* **1994**, 4, 1103.
- (28) Hariharan, R.; Biver, C.; Russel, W. B. To be submitted, 1996.
- (29) Li, J.; Caldwell, K. D.; Rapoport, N. *Langmuir* **1994**, 10, 4475.

- (30) Guenoun, P.; Davis, H. T.; Tirrell, M.; Mays, J. W. *Macromolecules* **1996**, *29*, 3965.
- (31) Qiu, X.; Wang, Z. *J. Colloid Interf. Sci.* **1994**, *167*, 294.
- (32) Watanabe, H.; Patel, S. S.; Argillier, J. F.; Parsonage, E. E.; Mays, J. W.; Dan-Brandon, N.; Tirrell, M. *Mat. Res. Soc. Symp. Proc.* **1992**, *249*, 255.
- (33) Merrington, A.; Yang, Z.; Meier, D. J. *68th ACS Colloid Surf. Symp.* **1994**.
- (34) Singh, N.; Karim, A.; Bates, F. S.; Tirrell, M.; Furusawa, K. *Macromolecules* **1994**, *27*, 2586.
- (35) de Gennes, P. G. *Scaling Concepts in Polymer Physics*, Cornell University: Ithaca, NY 1978.
- (36) Flory, P. J. *J. Chem. Phys.* **1949**, *17*, 303.
- (37) Brandrup, J.; Immergut, E. H. *Polymer Handbook*, 3rd ed.; Wiley Interscience: New York, 1989.
- (38) Flory, P. J. *Principles of Polymer Chemistry*, Cornell University: Ithaca, NY, 1953.
- (39) Davis, R. M.; Russel, W. B. *Macromolecules* **1987**, *20*, 518.
- (40) Mays, J.; Chen, R. Unpublished results, 1992.
- (41) Guenoun, P.; Lipsky, S.; Mays, J. W.; Tirrell, M. *Langmuir* **1996**, *12*, 1425.
- (42) Marko, J. F.; Rabin, Y. *Macromolecules* **1992**, *25*, 1503.
- (43) Wittmer, J.; Joanny, J. F. *Macromolecules* **1993**, *20*, 2691.
- (44) Hariharan, R.; Biver, C.; Russel, W. B. To be submitted, 1996.

MA9610065